19th Brazilian Congress of Thermal Sciences and Engineering
November 06th-10th, 2022, Bento Gonçalves - RS - Brazil

COMPARISON OF RANS, DES AND LES TURBULENCE MODELS TO DETERMINE DISCHARGE COEFFICIENTS OF AN ENGINE CYLINDER HEAD

Cristian Douglas da Silva
Universidade Federal de Santa Maria
douglas.silva@acad.ufsm.br

Jean Lucca Souza Fagundez
Universidade Federal de Santa Maria
jean.fagundez@acad.ufsm.br

Vinícius Rückert Roso
Universidade Federal de Santa Maria
vinicius.roso@mecanica.ufsm.br

Thompson Diórdinis Metzka Lanzanova
Universidade Federal de Santa Maria
lanzanova@mecanica.ufsm.br

Mario Eduardo Santos Martins
Universidade Federal de Santa Maria
mario@mecanica.ufsm.br

Abstract. *In view of recent international agreements on reducing greenhouse gas emissions, some groups advocate that the only solution is the total replacement of internal combustion engines by electric vehicles during the next few years. However, this change is a questionable alternative since the world energy matrix has high levels of non-renewable sources. A sustainable transition from internal combustion engines to hybrid and electrified solutions could be achieved with advanced combustion strategies and renewable fuels utilization. In this sense, the use of computational fluid dynamics (CFD) models is an important ally in the study of microscale phenomena, such as turbulence and its effects on combustion and engine efficiency. This paper intends to show the difference in the modeling and validation of a diesel engine cylinder head in a flow bench using three different turbulence numerical resolution methods, from the lowest to the highest complexity in the analysis of turbulence microscales: Reynolds Averaged Navier Stokes (RANS), Detached Eddy Simulation (DES) and Large Eddy Simulation (LES). For this purpose, an inlet valve of a diesel engine cylinder head was analyzed with forward air passage through several lift positions, from 1 to 10 mm, as well as the study of mesh independence. The discharge coefficients found by CFD modeling, when compared with those determined experimentally by a flow bench equipment, showed that the RANS, DES and LES models reached highly accurate results for all valve lifts. Due to the resolution method of each model, a greater difference in flow values and, consequently, discharge coefficients would be found for flows with high turbulence intensity. Thus, for cases where the flow has greater turbulence intensity, the LES model would be the most suitable for predicting experimental values, while the RANS model had its most suitable application for situations where lower mesh detail is needed or the flow presents lower turbulence intensity.*

Keywords: *computational fluid dynamics, turbulence, RANS, DES, LES*

1. INTRODUCTION

Internal combustion engines (ICE) are undergoing a moment of contestation due to the load of emissions they release into the atmosphere and the impact of this on climate change (The Economist, 2017). However, its use is widespread across the globe and there is no way to ban it in the short term without generating a crisis in transport and energy sectors. The supply and demand network that determines which form of energy is used in transport at each location is very complex and transitions must be done with caution (Kalghatgi, 2018). For this reason, safer than banning ICEs and replacing them overnight with electric vehicles is to develop them in such a way that polluting and greenhouse gases could be reduced until a smooth transition to a new energy matrix is achieved (Godazi Langeroudi et al., 2021; Oikawa et al., 2022). Improvements in internal combustion engines can be obtained in several ways: using alternative fuels; maximizing combustion efficiency; improving the design of engine components; among others (Wahono et al., 2021).

Following the path of improvement in engine component design, the development of intake manifolds is a focal point to increase engine performance and reduce exhaust emissions (Cui et al., 2015; Desantes et al., 2010). The intake port, by being connected to the cylinder, can directly affect the volume of air entering the combustion chamber, as well as the air velocity distribution and turbulence conditions in the chamber (Wahono et al., 2021). The inlet runner can influence the resonant frequencies of the manifold by varying its length or, to some extent, its diameter (Souza et al., 2019). Another point to consider, in addition to the shape of the intake runner, is the poppet valve (or valves) that open and close during engine operation, allowing air to enter. The closer the geometric air passage area and the effective air flow area are, the more efficient is the intake process. This area ratio is used to calculate the intake manifold discharge coefficient (C_D) (Heywood, 2018).

For the experimental determination of flow values through tubes and ducts of any nature, the most used equipment is the steady-state flow bench. By imposing a pressure gradient, the air that passes through the runners of an engine cylinder head, for example, will have its flow determined. Determining this flow allows the calculation of the discharge coefficient in the pipe, which makes this equipment an important tool for comparison between different designs and increased efficiency (El-Adawy et al., 2017; Wahono et al., 2019). Another form of experimental measurement used in a more recent study was developed specifically for determining the flow from the intake port to the cylinder with a film split-fiber probe. The objective was to identify, more faithfully than in a flow bench, the turbulence structures formed inside the cylinder after the passage of air through the port (Lepicovsky & Hatschbach, 2021). Regardless of the equipment, computational fluid dynamics (CFD) has been used to help experiments, seeking to reduce experimental costs without losing the necessary accuracy.

Numerical simulations in CFD software can predict the flow structures of a given fluid based on the boundary conditions chosen for the system. However, it is not uncommon for the mathematical models used to have a series of parameters that need to be adjusted for the model to be validated, that is, to be able to accurately predict an experimental result (Vítek et al., 2015). The challenge of 3D modeling lies in predicting the formation of turbulence eddies, which are highly dependent on the turbulence model used and the mesh refinement. Thus, information about turbulence is given, in most cases, only in a qualitative way (Basara et al., 2012). Furthermore, with the evolution of CFD techniques, there is currently more than one method for numerically solving fluid flow. Three of the best-known methods are: Reynolds Averaged Navier Stokes (RANS) (Wang & Hu, 2012); Detached Eddy Simulation (DES) (Basu et al., 2009); Large Eddy Simulation (LES) (Catellani et al., 2016; Ko et al., 2022). Little is explored, however, the difference in results between these numerical methods of turbulence resolution and whether there is a more appropriate method depending on the study and the boundary conditions used.

This paper seeks to compare the use of these numerical methods of turbulence resolution in a case study of air flow through the intake runner of a Diesel engine cylinder head. To determine the air flow, 4 different lift positions of the inlet valve were tested in direct air passage: 1 mm, 4 mm, 7 mm and 10 mm. A mesh independence study was also carried out in one of the cases to determine the level of mesh refinement capable of guaranteeing convergence. Experimental tests were carried out on all cases tested through a flow bench in order to test model validation, and the numerical resolution by CFD, using the software CONVERGE STUDIO 3.0, considered RANS, DES and LES methods.

2. METHODOLOGY

This chapter is divided into 3 subsections: First, tests were performed on the flow bench with a Hyundai HR 2.5 16V engine cylinder head. Subsequently, the geometry of the engine was elaborated through two softwares: SolidWorks® and CONVERGE STUDIO 3.0®. Finally, the CFD simulations were configured with the boundary conditions determined in the flow bench. Thus, the simulations analyzed the lift variations, flow direction change and the turbulence model.

2.1 Flow bench

Flow benches are equipment used to measure the steady-flow through several types of pipes and ducts, related or not to internal combustion engines. To calculate the discharge coefficient for a given geometry, controlled pressure and temperature parameters are used. Thus, the pressure gradient configured in the equipment forces air to pass through the

pipe and the output flow is read. Based on parameters such as the geometric air passage area and the effective air flow area, which considers the existing restrictions, it is possible to determine the discharge coefficient value, the impact that the restrictions cause on the flow and possible improvements to the geometry.

2.1.1 Flow bench specifications

Fig 1 shows the flow bench equipment that was used in the tests with the Hyundai HR 2.516V cylinder head in one of the analyzed positions, with dial indicators to determine the lift of the intake valve.

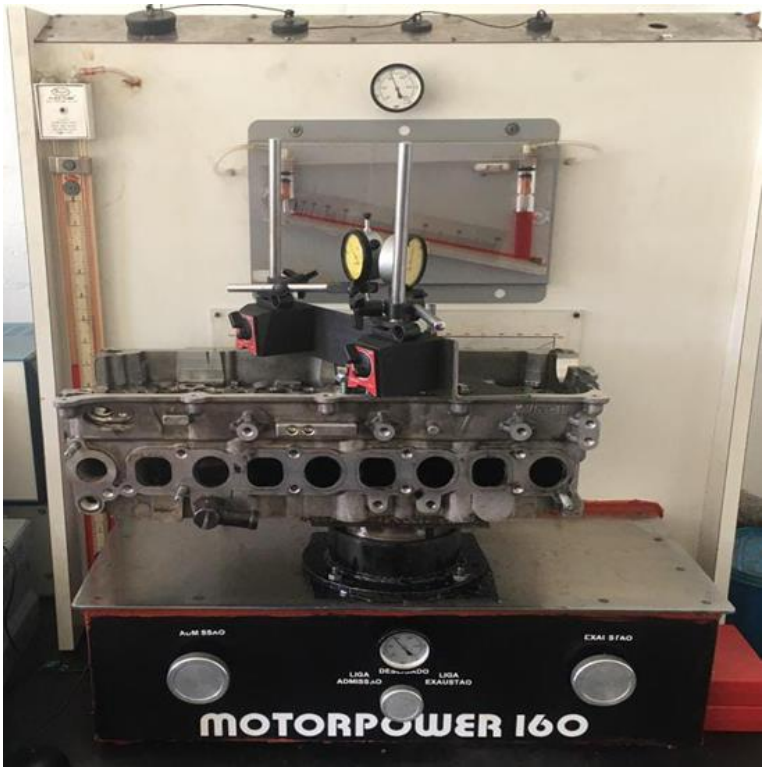

Figure 1. Flow bench structure with Hyundai HR 2.5 engine head positioned for testing.

For all tested lift positions, a pressure gradient of 2488.4 Pa (10 inches of H_2O) was imposed at 296.15 K (23 °C).

2.1.2 Experimental tests

To carry out the tests, a support with the same diameter as the cylinder of the Hyundai HR 2.5 16V engine was positioned between the flow bench air orifice and the cylinder head. The cylinder head was positioned on the support through nuts and bolts, with a gasket between them to ensure sealing. Then, a flange was used where the adjustment of the screws was responsible for opening and closing the inlet valve, changing the desired lift position, together with dial indicators in order to accurately quantify the lift.

2.2 Three-dimensional geometry model

The geometry depicted in this paper was created in SolidWorks® and exported for simulations in CONVERGE STUDIO 3.0®. The geometry includes the intake and exhaust runners from one of the cylinders of the Hyundai HR 2.5 16V engine, with part of the combustion chamber. From this, all the engine parts were grouped (intake and exhaust runners, cylinder and cylinder liner, valves, etc.) and all the geometry imperfections were corrected, such as: intersections, open edges, overlapping triangles, bad orientation of normal vectors and isolated triangles. The complete and the simplified geometries are both shown in Fig 2.

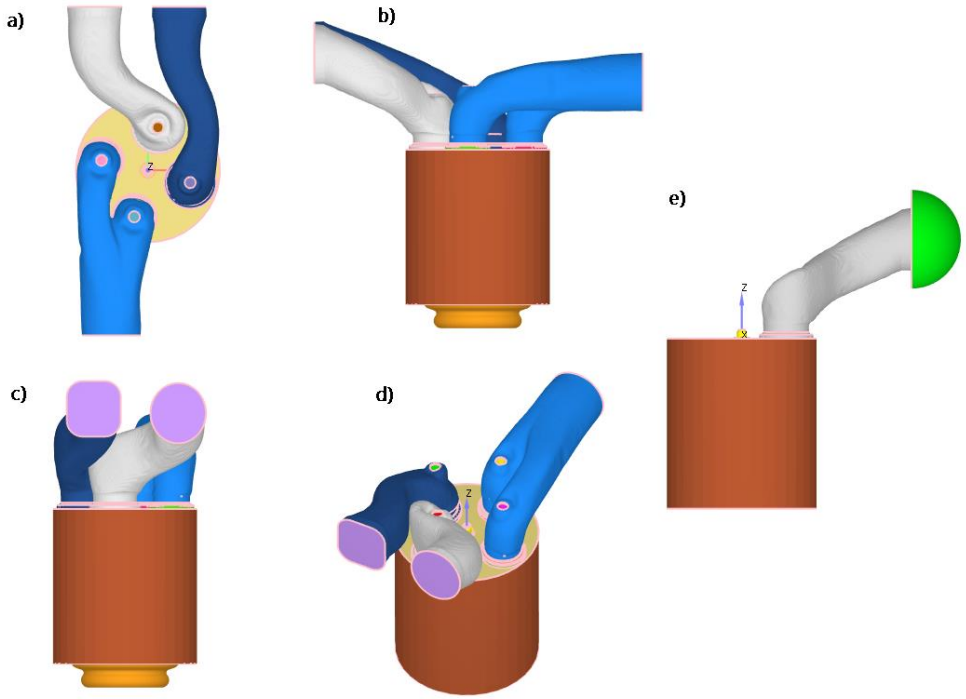

Figure 2. Complete cylinder and cylinder head geometry for the Hyundai HR 2.5 16V in: a) upper view; b) side view; c) front view; d) isometric view; and e) simplified inlet runner geometry for CFD simulations with direct airflow.

For the case study performed, only one of the inlet tubes was considered, with the grey color and greater curvature in Fig. 2. For the numerical resolution of airflow, the duct and cylinder must be modified to reflect the air inlet through the ports, as shown in Fig. 2 (e).

After finishing the simulation geometry, all input, output, moving mesh, boundaries, among others, are defined in the pre-processing. At defined times during the mesh numerical resolution, output files necessary for post-processing results are created. These output files allow the visualization of averaged two-dimensional results, such as in-cylinder pressure as a function of the crankshaft angle, or three-dimensional outputs that must be post-processed in a third-party software.

2.3 CFD simulations

With the digital geometries defined and the boundary conditions obtained through the flow bench tests, it was possible to configure the case setup for the RANS, DES and LES methods. All simulations considered air as an ideal gas and used a pressure-based PISO scheme to solve the Navier-Stokes equations. The equations for solving momentum, pressure, density, energy, among others, were kept at their default definitions in CONVERGE STUDIO 3.0®.

The base grid was selected based on mesh independence tests with RANS for turbulence resolution. Tab. 1 shows the tested mesh configurations for a 10 mm lift of the poppet valve.

Table 1. Base grid analysis for the mesh independence test.

Base grid size (dx, dy, dz)	Number of cells
20 mm	101
15 mm	240
10 mm	811
8 mm	1584
6 mm	3756
4 mm	12675
2 mm	101401
1 mm	811209

In addition to the base grid setup, adaptive mesh refinement (AMR) was also used based on a velocity magnitude sub-grid criterion in the X, Y and Z directions above 20 m/s.

In addition to typical output variables such as pressure, temperature and flow rate, turbulence variables such as turbulence kinetic energy (TKE) and turbulence dissipation rate (EPS) were also selected for post-processing.

The simulations were performed with minimum time step of $1 \cdot 10^{-6}$ s and maximum time step of $1 \cdot 10^{-4}$ s, during a total time of 0.01 s.

For the numerical resolution of turbulence, each method uses different models. With the RANS method, the selected model was the RNG (Renormalization Group) *k*-ε, recommended for internal combustion engines, that accounts for more scales of motion but can be less numerically stable. For the DES method, the turbulence model chosen was the DDES (Delayed Detached Eddy Simulation), a *k*-ω SST based model, which is better for low Re flows and have a good resolution of flow near walls, but is highly dependent on wall distance. Finally, for the LES method, the turbulence model selected was the Viscous One-Equation, that includes a transport equation for *k*, but does not have all its coefficients dynamically determined (Convergent Science, 2020).

2.4 Discharge coefficient

The discharge coefficient is defined as the ratio between the actual flow and the maximum (theoretical) flow that a given device can deliver (Heywood, 2018). For the calculation of the actual flow through a pipe with a poppet valve, the effective air flow area must be determined according to Eq. (1) (Blair, 1999),

$$A_R = \frac{\dot{m}\sqrt{\gamma R T_0}}{\gamma P_0 \left(\frac{P_T}{P_0}\right)^{\frac{1}{2}} \sqrt{\frac{2}{\gamma - 1}\left(1 - \left(\frac{P_T}{P_0}\right)^{\frac{\gamma-1}{\gamma}}\right)}} \tag{1}$$

where A_R is the effective air flow area, $\dot{m}$ is the mass flow of air, γ is the adiabatic expansion coefficient, R is the ideal gas universal constant, T_0 is the ambient temperature, P_0 is the intake runner pressure and P_T is the pressure after restriction.

The ratio between the actual flow and the theoretical flow can be translated by the ratio between the effective air flow area by the geometric air passage area, arriving at the discharge coefficient (C_D) value for the pipe, as shown by Eq. (2),

$$C_D = \frac{A_R}{A_G} \tag{2}$$

where A_G is the geometric air passage area.

Finally, as a way of comparing the experimental tests on the flow bench and the CFD models with RANS, DES and LES, the absolute error between C_D values was calculated, according to Eq. (3),

$$E_A = C_{D,e} - C_{D,s} \tag{3}$$

where $C_{D,e}$ is the experimental discharge coefficient at a given lift position and $C_{D,s}$ is de CFD calculated discharge coefficient for the same lift position.

3. RESULTS AND DISCUSSION

This chapter presents the simulation results in terms of mesh independence, in addition to the comparison of RES, DES and LES with data obtained experimentally in a flow bench for the air flow through a inlet valve from a Diesel engine.

3.1 Mesh independence

Before the comparative analysis between the results of each turbulence resolution method, it is important to define a grid size capable of guaranteeing the convergence of the simulations regardless of the mesh. The 10 mm inlet valve lift and the RANS method were used for this analysis. Fig. 3 shows the result in terms of air flow for the different grid sizes.

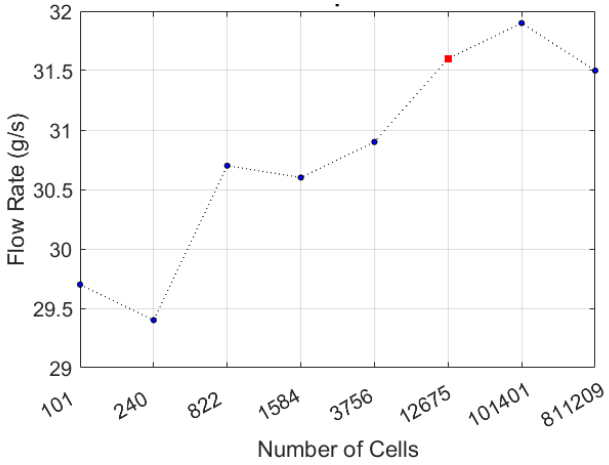

Figure 3. Mesh independence test for 20 to 1 mm mesh grid (from lower to higher number of cells).

The mesh independence test aims to find the minimum grid size (or minimum number of cells to be solved) so that the output values do not vary significantly. We observe, according to Fig. 3, that mesh independence is achieved with a 4 mm grid in X, Y and Z directions, with a mesh of 12675 cells. Thus, all simulations comparing RANS, DES and LES methods were performed using a 4 mm base grid size.

3.2 RANS, DES and LES comparison

Before proceeding with the results comparison, it is important to emphasize that the case study considers a specific scenario, with a low-pressure gradient and, consequently, low air flow values. Therefore, the objective was to analyze only the differences in the resolution process used by each method and determine if one of them is more appropriate for analysis of this type. All of the following results show from the beginning of the air passage through the inlet runner to a moment where the flow is stationary, at 0.01 s.

Fig. 4 shows the pressure and temperature variation in the cylinder region.

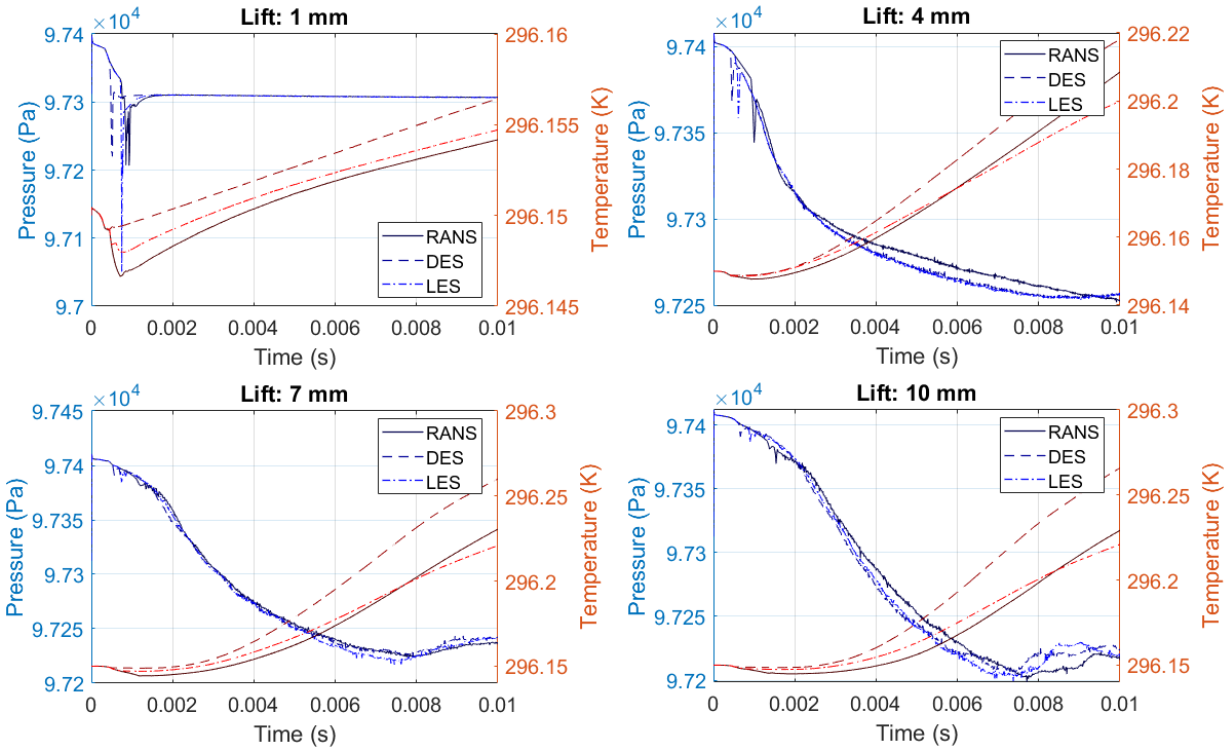

Figure 4. Pressure and temperature variation in the cylinder region for different valve lifts. Pressure curves, in blue, are read on the left axis, and temperature curves, in red, are read on the right axis.

Regarding the pressure, it can be noticed very similar behavior between the three methods, with a slight reduction in the pressure value, intensified as the valve opening lift increases. Temperature, on the other hand, has a different profile for each method. The maximum increase value of 0.125 K, which reflects the increase in kinetic energy due to the increase in air velocity across the valve restriction, is higher for the DES method, while the RANS and LES methods yield closer results.

The difference in magnitude or percentage of values, both pressure and temperature, does not determine a relevant difference between RANS, DES and LES.

Fig. 5 shows the results for variation of turbulence kinetic energy (TKE) and turbulence dissipation rate (EPS) in the cylinder region.

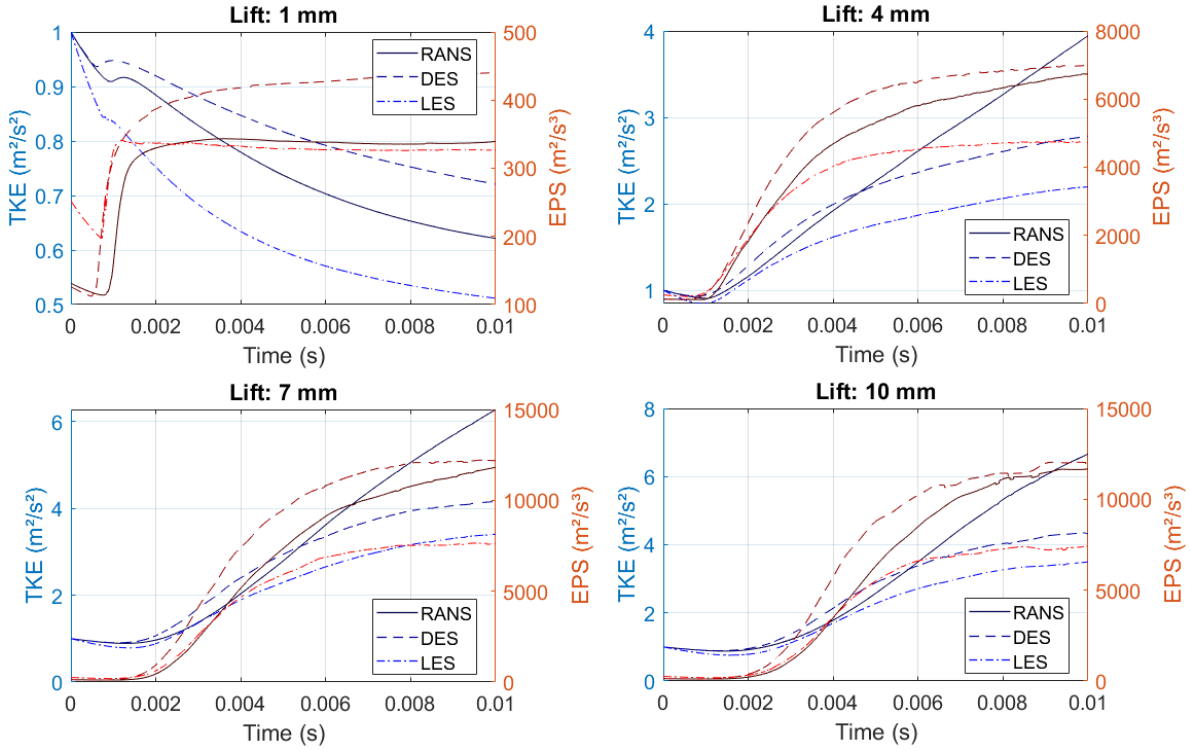

Figure 5. TKE and EPS variation in the cylinder region for different valve lifts. TKE curves, in blue, are read on the left axis, and EPS curves, in red, are read on the right axis.

TKE results, also known as the *k* variable of turbulence models, show the average kinetic energy per unit mass associated with eddies in turbulent flows. In the case studied, TKE can be produced mainly by fluid shear and friction. It can be noticed that, for the smallest valve lift, TKE decreases, indicating a tendency of turbulence reduction over time due to the low air flow. In all other cases, the kinetic energy per unit of mass increases the greater the valve lift, something expected due to the air flow increase. Among the methods, RANS predicts twice the TKE value of LES in the last time step, with DES indicating intermediate values (closer to LES). However, these differences in TKE and EPS magnitudes between the models do not have a significant influence in terms of heat transfer.

Regarding turbulence dissipation rate, the ε variable in turbulence models, there is a connection between the results found for EPS and the slight increase in temperature. This is because the kinetic energy that dissipates from the eddies is released as thermal energy, which increases the temperature of the fluid. For this reason, at 1 mm valve lift condition, one can see a decrease in TKE and an increase in EPS, which explains why the temperature grows in Fig. 4. In all other poppet valve opening conditions, TKE and EPS increase, as the air flow is greater and there is greater turbulence and energy dissipation from the eddies after passing through the restriction.

Fig. 6 shows a comparison, for the RANS method, between the magnitude of fluid velocity and the turbulent velocity for 1 mm valve lift and 10 mm valve lift conditions.

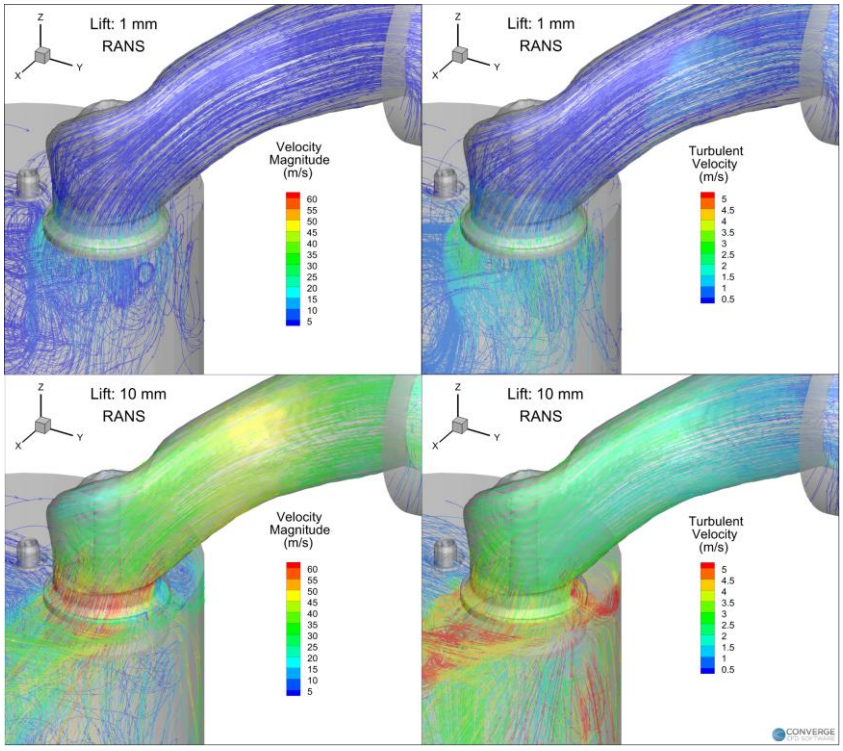

Figure 6. Velocity Magnitude and Turbulent Velocity comparison for 1 mm valve lift and 10 mm valve lift with RANS.

The images in Fig. 6 help to explain the previous results of TKE and EPS in the cylinder region, showing that, for 1 mm valve lift, the fluid velocity at the valve restriction has values between 20 and 40 m/s, while at 10 mm valve lift, the velocity can exceed 60 m/s. The consequence is clearly shown in turbulent velocity, a variable that is a function of TKE, and is much more intense in the cylinder region for the 10 mm valve lift condition.

Fig. 7 shows the results of the air flow predicted by each method.

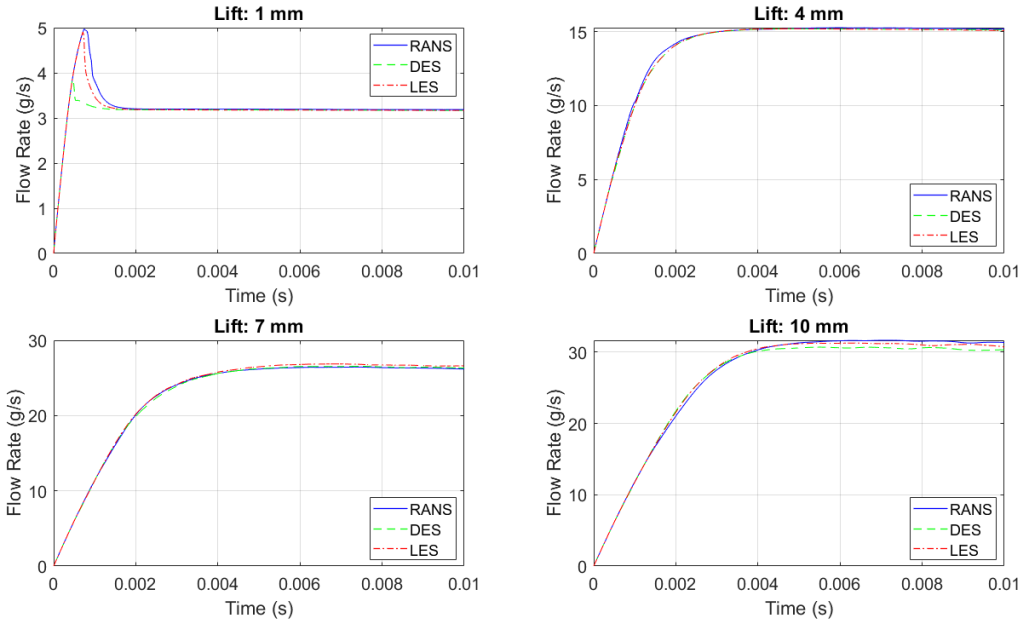

Figure 7. Flow rate from the intake runner region to the cylinder region.

The predicted results for air flow show that, for any method of numerical resolution of turbulence in the case study performed, the final air flow rate is almost the same. This may occur because the pressure gradient is small and the passage of air through the valve restriction does not have a significant impact on turbulence to the point that the differences

between each method could be more highlighted. This similarity is also reflected in the calculation of the discharge coefficient (C_D) values, shown next.

3.3 Discharge coefficient comparison

After determining the flow rate through the restriction in each lift condition, the pressure gradient and the temperature, it was possible to calculate the effective air flow area with Eq. (1). Then, through Eq. (2), discharge coefficient values were calculated and filled in Tab. 2 for the flow bench and for RANS, DES and LES, with the respective computational prediction errors compared to the experimental values.

Table 2. Discharge coefficient (C_D) comparison between flow bench and RANS, DES and LES turbulence resolution methods.

Valve Lift Position (mm)	Flow Bench C_D	RANS C_D	DES C_D	LES C_D	RANS Error (%)	DES Error (%)	LES Error (%)
1	0.073	0.069	0.068	0.068	5.55%	6.47%	6.47%
4	0.324	0.327	0.327	0.327	-0.79%	-0.99%	-0.85%
7	0.544	0.569	0.571	0.578	-4.57%	-5.06%	-6.23%
10	0.669	0.681	0.658	0.667	-1.68%	1.71%	0.33%

Absolute errors were below 7% for 1 mm and 7 mm valve lift conditions, while for 4 mm and 10 mm, error values were below 2% for any of the three methods. Thus, for the case study considered, any of the numerical methods of turbulence resolution proved to be adequate, reaching air flow values very close to the experimental ones. Due to the proposal of each method, it can be expected that greater differences between results will be observed in cases where turbulence intensity is much higher and the number of mesh cells needed would exceed millions. Thus, results will be similar for RANS, DES and LES in cases with low turbulence intensity and a mesh grid that does not require much refinement.

The results found also justify the more frequent use of CFD models, often replacing experiments, due to their high accuracy. Furthermore, given the current processing capacity of computers, 3D computer models, once time consuming due to their high computational demand, can currently be solved in a few hours. These benefits underscore why CFD models are deemed as an essential tool in the research and development of high-performance internal combustion engines and will be part of the solution to extend the life of these thermal machines during the transition to electric vehicles.

4. CONCLUSIONS

The study carried out sought to compare three methods for solving turbulence in computational fluid dynamics models, RANS, DES and LES. For this analysis, the cylinder head of a Hyundai HR 2.5 16V diesel engine underwent experimental tests on a flow bench and was digitally reproduced in 3D geometry, aiming at the CFD models validation by comparing the values of the discharge coefficient of one of the engine intake runners to the cylinder. After determining the grid required for mesh independence, the simulations performed reached the following results:

- The pressure drop in the cylinder region was similarly predicted with the RANS, DES and LES methods;
- The relationship between cylinder temperature variation was consistent with TKE and EPS results, with RANS predicting higher values of kinetic energy in the formed eddies and greater dissipation rate of this energy, followed by DES and LES;
- Due to the low experimental pressure gradient, the three turbulence resolution methods predicted very similar values of air flow rate in the four valve lift conditions tested;
- The discharge coefficients predicted by each method were very similar and with small error compared to the experimental values, less than 7% in the 1 mm and 7 mm valve lifts and less than 2% in the 4 mm and 10 mm valve lifts;

Given their accuracy, the potential of CFD models is pointed out as tools capable of testing and improving internal combustion engines, reaching more efficient machines with less impact on the environment.

5. ACKNOWLEDGEMENTS

The authors gratefully acknowledge the financial support of Rota Program 2030 - Segment V - FUNDEP (project number: 27192.01.01/2020.06-00). The authors also thank CNPq, CAPES and FAPERGS for the financial support for the laboratory activities.

6. REFERENCES

Basara, B., Krajnovi, S., Girimaji, S., & Pavlovic, Z. (2012). Near-Wall Formulation of the Partially Averaged Navier Stokes Turbulence Model. *Https://Doi.Org/10.2514/1.J050967*, *49*(12), 2627–2636. https://doi.org/10.2514/1.J050967

Basu, D., Das, K., Painter, S. L., Howard, L. O., & Green, S. T. (2009). Assessment of DES Multiscale Turbulence Models for Prediction of Flow and Heat Transfer in an Axial-Channel Rod Configuration. *International Conference on Nuclear Engineering, Proceedings, ICONE*, *2*, 425–438. https://doi.org/10.1115/ICONE16-48515

Berselli, L. C. (Luigi C.), Iliescu, T. (Traian), & Layton, W. J. (William J.). (2006). *Mathematics of large eddy simulation of turbulent flows*. Springer.

Blair, G. P. (1999). *Design and Simulation of Four-Stroke Engines*. Society of Automotive Engineers, Inc.

Catellani, C., Cazzoli, G., Falfari, S., Forte, C., & Bianchi, G. M. (2016). Large Eddy Simulation of a Steady Flow Test Bench Using OpenFOAM®. *Energy Procedia*, *101*, 622–629. https://doi.org/10.1016/J.EGYPRO.2016.11.079

Convergent Science. (2020). *CONVERGECFD MANUAL SERIES CONVERGE MANUAL v3.0*.

Cui, L., Wang, T., Lu, Z., Jia, M., & Sun, Y. (2015). Full-parameter approach for the intake port design of a four-valve direct-injection gasoline engine. *Journal of Engineering for Gas Turbines and Power*, *137*(9). https://doi.org/10.1115/1.4029686/374019

Desantes, J. M., Galindo, J., Guardiola, C., & Dolz, V. (2010). Air mass flow estimation in turbocharged diesel engines from in-cylinder pressure measurement. *Experimental Thermal and Fluid Science*, *34*(1), 37–47. https://doi.org/10.1016/J.EXPTHERMFLUSCI.2009.08.009

El-Adawy, M., Heikal, M. R., Aziz, A. R. A., Siddiqui, M. I., & Abdul Wahhab, H. A. (2017). Experimental study on an IC engine in-cylinder flow using different steady-state flow benches. *Alexandria Engineering Journal*, *56*(4), 727–736. https://doi.org/10.1016/J.AEJ.2017.08.015

Godazi Langeroudi, A. S., Sedaghat, M., Pirpoor, S., Fotouhi, R., & Ghasemi, M. A. (2021). Risk-based optimal operation of power, heat and hydrogen-based microgrid considering a plug-in electric vehicle. *International Journal of Hydrogen Energy*, *46*(58), 30031–30047. https://doi.org/10.1016/J.IJHYDENE.2021.06.062

Heywood, John. B. (2018). *Internal Combustion Engine Fundamentals-McGraw-Hill Education (2018)*.

Kalghatgi, G. (2018). Is it really the end of internal combustion engines and petroleum in transport? *Applied Energy*, *225*, 965–974. https://doi.org/10.1016/J.APENERGY.2018.05.076

Ko, I., Kim, J., & Min, K. (2022). Understanding the effect of turbulent flow on the combustion cyclic variation in a spark ignition engine using Large-Eddy simulation. *Fuel*, *322*, 123773. https://doi.org/10.1016/J.FUEL.2022.123773

Lepicovsky, J., & Hatschbach, P. (2021). Introductory measurements of in-cylinder flow past intake valve ports with a film split-fiber probe. *Flow Measurement and Instrumentation*, *80*, 102003. https://doi.org/10.1016/J.FLOWMEASINST.2021.102003

Oikawa, M., Kojiya, Y., Sato, R., Goma, K., Takagi, Y., & Mihara, Y. (2022). Effect of supercharging on improving thermal efficiency and modifying combustion characteristics in lean-burn direct-injection near-zero-emission hydrogen engines. *International Journal of Hydrogen Energy*, *47*(2), 1319–1327. https://doi.org/10.1016/J.IJHYDENE.2021.10.061

Sagaut, P., Deck, S., Terracol, M., & World Scientific (Firm). (2013). *Multiscale and multiresolution approaches in turbulence : LES, DES and hybrid RANS/LES methods : applications and guidelines*. Imperial College Press.

Souza, G. R. de, Pellegrini, C. de C., Ferreira, S. L., Soto Pau, F., & Armas, O. (2019). Study of intake manifolds of an internal combustion engine: A new geometry based on experimental results and numerical simulations. *Thermal Science and Engineering Progress*, *9*, 248–258. https://doi.org/10.1016/J.TSEP.2018.12.003

The Economist. (2017). *The death of the internal combustion engine | The Economist*. 12th to 18th August. https://www.economist.com/leaders/2017/08/12/the-death-of-the-internal-combustion-engine

Vítek, O., Tichánek, R., & Hatschbach, P. (2015). Application of LES, PANS and RANS to a Case of Intake Channel Steady Flow Test Bench. *Middle Euro. Constr. Design Car.*, 14–23. https://doi.org/10.1515/mecdc-2015-0011

Wahono, B., Jwa, K., & Lim, O. (2019). A Study on In-Cylinder Flow of Small Engine Using Steady-State Flow Benches. *Energy Procedia*, *158*, 1856–1862. https://doi.org/10.1016/J.EGYPRO.2019.01.432

Wahono, B., Setiawan, A., & Lim, O. (2021). Effect of the intake port flow direction on the stability and characteristics of the in-cylinder flow field of a small motorcycle engine. *Applied Energy*, *288*, 116659. https://doi.org/10.1016/J.APENERGY.2021.116659

Wang, J., & Hu, X. (2012). Application of RNG k-ε Turbulence Model on Numerical Simulation in Vehicle External Flow Field. *Applied Mechanics and Materials*, *170–173*, 3324–3328. https://doi.org/10.4028/WWW.SCIENTIFIC.NET/AMM.170-173.3324

7. RESPONSIBILITY NOTICE

The authors are the only responsible for the printed material included in this paper.